



HAL
open science

Regression-based ranking of pathogen strains with respect to their contribution to natural epidemics

Samuel S. Soubeyrand, Charlotte Tollenaere, Emilie Haon-Lasportes,
Anna-Liisa Laine

► **To cite this version:**

Samuel S. Soubeyrand, Charlotte Tollenaere, Emilie Haon-Lasportes, Anna-Liisa Laine. Regression-based ranking of pathogen strains with respect to their contribution to natural epidemics. PLoS ONE, 2014, 9 (1), 10.1371/journal.pone.0086591 . hal-02630309

HAL Id: hal-02630309

<https://hal.inrae.fr/hal-02630309>

Submitted on 27 May 2020

HAL is a multi-disciplinary open access archive for the deposit and dissemination of scientific research documents, whether they are published or not. The documents may come from teaching and research institutions in France or abroad, or from public or private research centers.

L'archive ouverte pluridisciplinaire **HAL**, est destinée au dépôt et à la diffusion de documents scientifiques de niveau recherche, publiés ou non, émanant des établissements d'enseignement et de recherche français ou étrangers, des laboratoires publics ou privés.

Regression-Based Ranking of Pathogen Strains with Respect to Their Contribution to Natural Epidemics

Samuel Soubeyrand^{1*}, Charlotte Tollenaere^{2‡}, Emilie Haon-Lasportes¹, Anna-Liisa Laine²

1 UR546 Biostatistics and Spatial Processes, INRA, Avignon, France, **2** Metapopulation Research Group, Department of Biosciences, University of Helsinki, Helsinki, Finland

Abstract

Genetic variation in pathogen populations may be an important factor driving heterogeneity in disease dynamics within their host populations. However, to date, we understand poorly how genetic diversity in diseases impact on epidemiological dynamics because data and tools required to answer this questions are lacking. Here, we combine pathogen genetic data with epidemiological monitoring of disease progression, and introduce a statistical exploratory method to investigate differences among pathogen strains in their performance in the field. The method exploits epidemiological data providing a measure of disease progress in time and space, and genetic data indicating the relative spatial patterns of the sampled pathogen strains. Applying this method allows to assign ranks to the pathogen strains with respect to their contributions to natural epidemics and to assess the significance of the ranking. This method was first tested on simulated data, including data obtained from an original, stochastic, multi-strain epidemic model. It was then applied to epidemiological and genetic data collected during one natural epidemic of powdery mildew occurring in its wild host population. Based on the simulation study, we conclude that the method can achieve its aim of ranking pathogen strains if the sampling effort is sufficient. For powdery mildew data, the method indicated that one of the sampled strains tends to have a higher fitness than the four other sampled strains, highlighting the importance of strain diversity for disease dynamics. Our approach allowing the comparison of pathogen strains in natural epidemic is complementary to the classical practice of using experimental infections in controlled conditions to estimate fitness of different pathogen strains. Our statistical tool, implemented in the R package *StrainRanking*, is mainly based on regression and does not rely on mechanistic assumptions on the pathogen dynamics. Thus, the method can be applied to a wide range of pathogens.

Citation: Soubeyrand S, Tollenaere C, Haon-Lasportes E, Laine A-L (2014) Regression-Based Ranking of Pathogen Strains with Respect to Their Contribution to Natural Epidemics. *PLoS ONE* 9(1): e86591. doi:10.1371/journal.pone.0086591

Editor: Raya Khanin, Memorial Sloan Kettering Cancer Center, United States of America

Received: July 23, 2013; **Accepted:** December 13, 2013; **Published:** January 31, 2014

Copyright: © 2014 Soubeyrand et al. This is an open-access article distributed under the terms of the Creative Commons Attribution License, which permits unrestricted use, distribution, and reproduction in any medium, provided the original author and source are credited.

Funding: A-L Laine acknowledges funding from the Academy of Finland (Grant numbers 250444, 136393, 133499) and European Research Council (PATHEVOL; 281517). S Soubeyrand acknowledges funding from the French National Research Agency (EMILE project) and the European Union Seventh Framework Programme (PLANTFOODSEC, 261752). The funders had no role in study design, data collection and analysis, decision to publish, or preparation of the manuscript.

Competing Interests: The authors have declared that no competing interests exist.

* E-mail: Samuel.Soubeyrand@avignon.inra.fr

‡ Current address: UMR Résistance des Plantes aux Bioagresseurs (IRD-CIRAD-UM2), IRD, Montpellier, France

Introduction

Development of epidemiological models has been driven by the need to understand and predict the dynamics, invasion, and persistence of plant and animal diseases [1–3]. The inherent variable nature of epidemics and heterogeneous spatial distribution of pathogens in their host populations has presented a challenge for this work [4,5]. While variation in epidemics caused by abiotic environmental variation is relatively well understood [6,7], quantifying the effect of intraspecific diversity in pathogen populations on epidemic rates has remained a challenge. This is non-trivial as diversity in traits affecting infection and transmission is a ubiquitous feature of pathogen populations [8].

Until recently, the scarcity of suitable genetic markers has impeded the study of variation in pathogen populations [9,10]. However, with the development of Next Generation Sequencing, genetic tools are becoming increasingly available for parasites [11–13]. Molecular tracking of pathogen strains has the potential to identify disease transmission pathways across a variety of geographic scales [14]. At the very fine-scale of within host populations, molecular tools can reveal heterogeneities in

transmission generated by differences in infectivity and subsequent growth and reproduction of different parasite strains [8], and their interactions with their hosts (genotype-by-genotype interactions; [15,16]) and environment (genotype-by-environment interactions; [17,18]).

Linking genetic pathogen data to epidemiological dynamics allows unraveling the role of pathogen intraspecific diversity in disease dynamics but this is currently limited by the availability of suitable analytical tools. Among the challenges to overcome in the development of these tools are: (i) The scarcity of data required to fit multi-strain dynamical models; (ii) The change of scale in the resolution from epidemiological data to the resolution of pathogen genetic data; and (iii) The ambiguity in the effect of the heterogeneity in pathogen strains, as discussed above. Here, we present an exploratory analysis tool based on data transformation, linear regression and kernel smoothing to assign ranks to different pathogen strains with respect to epidemiological spread, and we analyze whether this ranking is significant. The linear regression links epidemiological data (response variable) to genetic data (explanatory variables), and the kernel smoothing allows the scale of genetic data to be matched with the scale of epidemiological

data. We apply our model to (i) data obtained under a statistical stochastic model, (ii) data obtained under a multi-strain mechanistic model (original model), and (iii) fine-scale within-season epidemiological data and genetical characterization of pathogen samples collected for the powdery mildew naturally infecting *Plantago lanceolata* in the archipelago of Finland. A recently developed protocol for field sampling of pathogen strains and Single Nucleotide Polymorphism (SNP) genotyping panel [19] allows a multilocus characterization of genetic content and subsequent distinction of different pathogen strains co-occurring within the same natural epidemic in this pathosystem.

Materials and Methods

Example of Field Data

Studied pathosystem. *Podosphaera plantaginis* (Castagne; U. Braun & S. Takamatsu) is a fungal pathogen specific to the ribwort plantain *Plantago lanceolata*. This species has been studied in the Åland archipelago (southwestern Finland), with long-term data evidencing metapopulation dynamics [20,21]. *Po. plantaginis* belongs to the family of powdery mildews (Erysiphales, Ascomycete). These obligate pathogens develop conspicuous white-greyish mycelia on the surface of their host leaves and only penetrate the host tissue through feeding structures named haustoria. Continuous production of asexual spores named conidia leads to the succession of various overlapping asexual cycles during the summer (generation time varying between one and two weeks under controlled conditions). The powdery mildew population crashes during the winter due to a lack of living host tissue, but reinitiation of the epidemics in the following spring is enabled by the germination of sexual resting structures named chasmothecia.

Epidemiological data. Small-scale data were collected during the summer 2011 within one *Pl. lanceolata* meadow (ID 609) located in the Eckero part of the Åland archipelago (Neither the host plant nor the pathogen is protected species and Finnish legislation (Jokamiehenoikeus) allows the sampling of wild species to everyone). This *Pl. lanceolata* population (approx. 2400 m²) was visited weekly between July 18 and August 25 (week 29 to 34), except on week 33 (five observations in total). Pattern of infection within host populations is known to be highly aggregated in this pathosystem [22]. Consequently, the survey was performed by dividing the studied location into 122 squared grid cells of 9 m². Every week, each cell was visually inspected, and the number of host leaves infected by the powdery mildew was recorded.

Genetic data. On the last day of the survey (last week of August), 45 infected leaves were sampled for genetic characterization. Samples were chosen from the different infected cells so that, in each cell, the number of collected samples was approximately related to the disease intensity. Genotyping of the fungal pathogen for 27 SNP markers was performed as described in [19]. This methodology consists of direct genotyping (no purification step) of the total fungal material found on one infected leaf and allows to detect whether infection of the leaf was caused by a unique vs multiple fungal strains [19]. Clear multilocus data obtained from unique infections were used to define the different fungal strains circulating within the population and to attribute each sample to a particular fungal strain. Most of the mixed-genotype infections could be assigned to a mix of two identified strains whereas few remained unattributed and were removed from the dataset.

Regression Model for the Analysis of Strain Contributions

Consider a host population covering a spatial domain divided into I similar grid cells. The cells are labelled by $i \in \{1, \dots, I\}$.

Two types of observations are made: epidemiological observations and pathogen genetic observations. The epidemiological data are pathogen intensities $Y_i(t)$ in cells $i \in \{1, \dots, I\}$ at times $t \in \{t_1, t_2\}$. The pathogen genetic data observed at time t_2 are J samples randomly collected in the grid cells and classified into a set of S strains. The label $j \in \{1, \dots, J\}$ is used to identify the samples. The label $s \in \{1, \dots, S\}$ is used to identify the strains. For each sample j , i_j is the cell where j was collected and s_j is the strain of j , and $\mathcal{I} = \{i_j : j = 1, \dots, J\} \subset \{1, \dots, I\}$ is the set of cells containing genetic samples. We introduce the variable Z_i satisfying:

$$Z_i = \log \left(\frac{1 + Y_i(t_2)}{1 + Y_i(t_1)} \right). \quad (1)$$

Z_i is built to characterize the growth of the epidemic in cell i between times t_1 and t_2 (the growth can be negative; see Discussion for other Z_i 's constructions). We assume that Z_i depends on the strains that are locally present at time t_2 in the following way:

$$Z_i = \left(\sum_{s=1}^S p_i(s) z(s) \right) + \eta_i, \quad (2)$$

where $p_i(s) \in [0, 1]$ is the proportion of strain s in cell i , $z(s) \in \mathbb{R}$ is the intrinsic growth rate of strain s ($z(s) = \mathbb{E}\{Z_i | p_i(s) = 1\}$ is the expectation of Z_i if only strain s is in cell i), and η_i is a centered normal random noise (η_1, \dots, η_I are assumed to be independent).

The model (2) can be viewed as a regression linear model where Z_i is the response variable, $\{p_i(1), \dots, p_i(S)\}$ is the vector of explanatory variables and $\{z(1), \dots, z(S)\}$ are the regression coefficients. Ranking the pathogen strains with respect to their contributions to field epidemics is achieved by ranking the coefficients $z(s)$, $s = 1, \dots, S$.

Approximation of the Regression Model

In model (2), the explanatory variables $p_i(s)$ ($i = 1, \dots, I$, $s = 1, \dots, S$) are not observed. However, using the pathogen genetic data and a kernel smoothing technique, the proportions $p_i(s)$ can be estimated and plugged in Equation (2). Let $\hat{p}_i(s)$ be an unbiased estimate of $p_i(s)$, i.e. $\mathbb{E}\{\hat{p}_i(s)\} = p_i(s)$, we replace the model (2) by the following approximate regression model:

$$Z_i = \left(\sum_{s=1}^S \hat{p}_i(s) z(s) \right) + \varepsilon_i, \quad (3)$$

where ε_i is a centered normal random noise with variance σ^2 ($\varepsilon_1, \dots, \varepsilon_I$ are assumed to be independent). The term ε_i is a noisy version of η_i because of the difference between $p_i(s)$ and $\hat{p}_i(s)$. We ignore the eventual dependence in the ε_i to keep the model simple (since it is only used like an exploratory tool) but such a dependence could be taken into account; see Discussion. In the model (3), we used the following weighted estimate of $p_i(s)$:

$$\hat{p}_i(s) = \frac{\sum_{i' \in \mathcal{I}} w_{i' i} p_{i'}^{obs}(s)}{\sum_{i' \in \mathcal{I}} w_{i' i}}, \quad (4)$$

where $w_{i' i}$ is the weight of pathogen samples collected in cell i' to estimate the proportion of strain s in cell i , $p_{i'}^{obs}(s)$ is the observed proportion of strains s in cell $i' \in \mathcal{I}$,

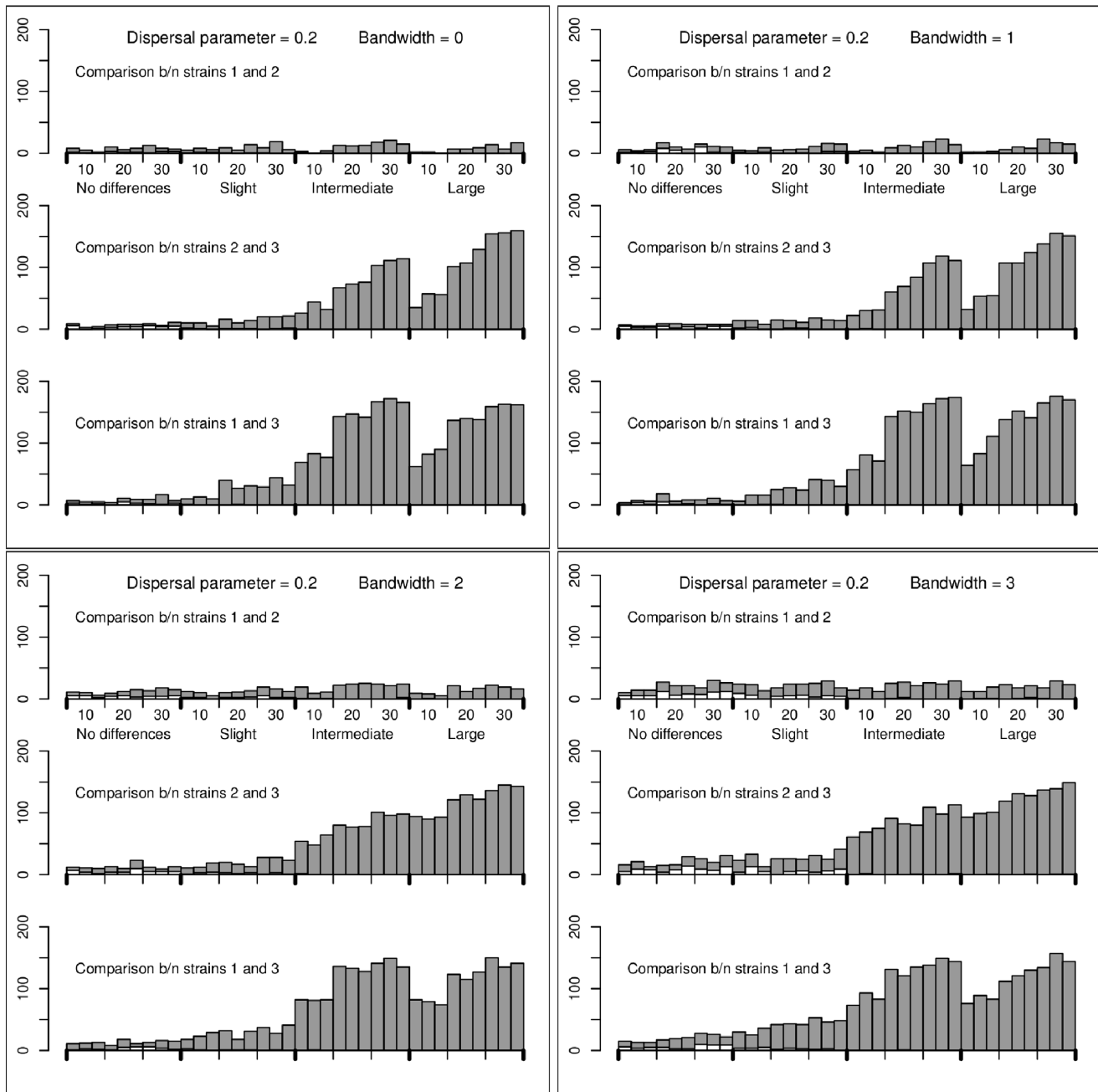


Figure 1. Numbers of test rejections for simulations performed under the mechanistic model with dispersal parameter $\gamma=0.2$. Grey bars: number of times that the null hypothesis was rejected and that the alternative was true; White bars: number of times that the null hypothesis was rejected and that the alternative was wrong. The rejection threshold was fixed at $0.05/3$ (using Bonferroni's correction). The number of sampling sites and the differences in the fitness coefficients are given under the x-axis of the top panels. Moreover, between each consecutive ticks, there are three bars corresponding, from left to right, to 1, 5 and 10 collected samples per sampling site. The results are provided for the bandwidth values $b=0$ (top left), $b=1$ (top right), $b=2$ (bottom left) and $b=3$ (bottom right). doi:10.1371/journal.pone.0086591.g001

$$p_{i'}^{obs}(s) = \frac{\sum_{j=1}^J \mathbb{1}(i_j = i' \text{ and } s_j = s)}{\sum_{j=1}^J \mathbb{1}(i_j = i')}$$

and $\mathbb{1}$ is the indicator function ($\mathbb{1}(E)=1$ if event E holds, zero otherwise). The denominator in Equation (4) ensures that the sum

of the estimated proportions $\hat{p}_i(s)$ over s is equal to one. We used a kernel form for $w_{i'}$ to give positive weights to samples collected in neighbor cells:

$$w_{i'} = K\left(\frac{d(i,i')}{b}\right) \tag{5}$$

where $d(i,i')$ is the distance between the centers of cells i and i' , K

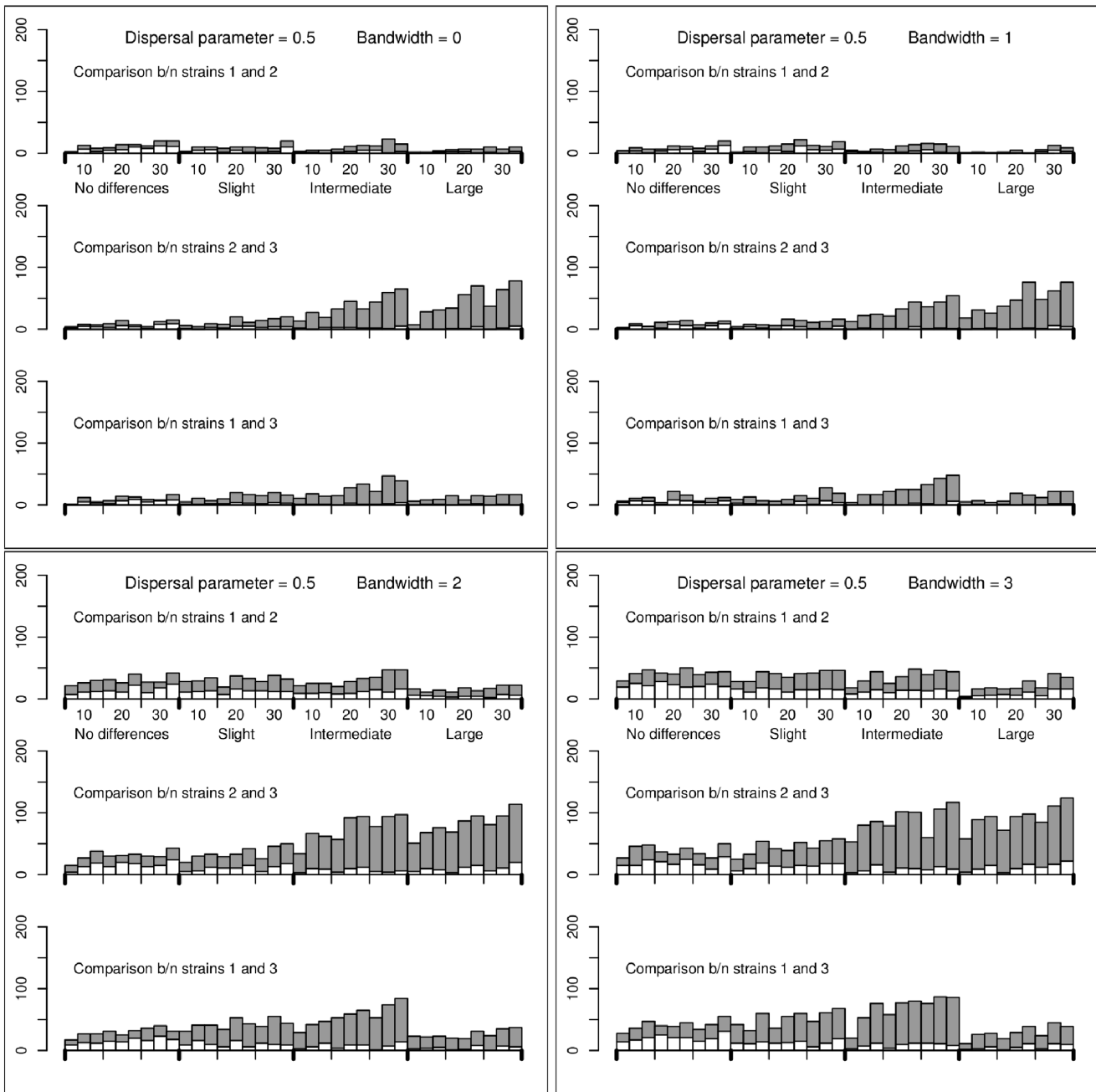


Figure 2. Numbers of test rejections for simulations performed under the mechanistic model with dispersal parameter $\gamma=0.5$. Grey bars: number of times that the null hypothesis was rejected and that the alternative was true; White bars: number of times that the null hypothesis was rejected and that the alternative was wrong. The rejection threshold was fixed at $0.05/3$ (using Bonferroni's correction). The number of sampling sites and the differences in the fitness coefficients are given under the x-axis of the top panels. Moreover, between each consecutive ticks, there are three bars corresponding, from left to right, to 1, 5 and 10 collected samples per sampling site. The results are provided for the bandwidth values $b=0$ (top left), $b=1$ (top right), $b=2$ (bottom left) and $b=3$ (bottom right). doi:10.1371/journal.pone.0086591.g002

is the quadratic kernel $K(u)=(1-u^2)\mathbb{1}(0\leq u\leq 1)$, and b is a bandwidth determining the extent of the kernel and, consequently, the number of observed proportions $p_i^{obs}(s)$ used to estimate each true proportion $p_i(s)$. By convention, under the case $b=0$, $w_{ii'}=1$ if $i=i'$ and zero otherwise.

In kernel smoothing, the choice of the bandwidth b corresponds to a trade-off between bias and variance of the estimates [23,24]. Smaller the bandwidth, smaller the bias and larger the variance.

Larger the bandwidth, larger the bias and smaller the variance. In the context that we are considering here, a too small bandwidth with respect to the amount of information available in the data may lead to strongly varying estimates of the strain proportions and, therefore, to state that a difference in the parameters $z(s)$ is significant whereas it is not. Conversely, when the bandwidth is increased, the estimated proportions of strains tend to be homogeneous in space and, therefore, we will not be able to

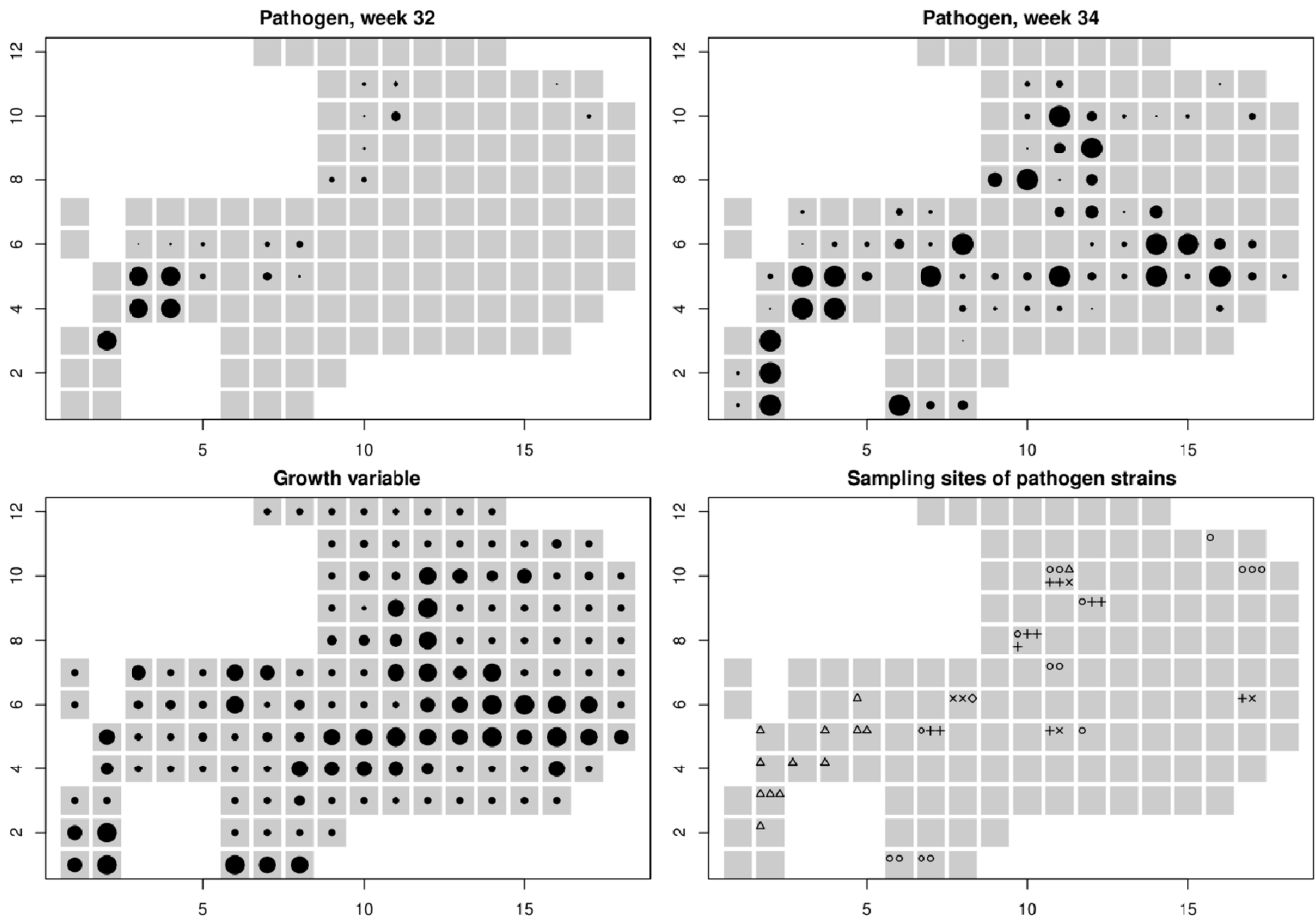


Figure 3. Powdery mildew data and growth variable in a patch of *Plantago lanceolata* in the Åland islands. In all the panels the grey squares represent the grid cells covering the host population. Top panels: number of infected leaves in 9m² square cells at weeks 32 (left) and 34 (right) of year 2011 (dot size proportional to number of infected leaves that ranges between 0 and 137). The axis scales indicate the number of the cell from the most bottom-left cell. Bottom left: Growth variable Z_i (dot size linear in Z_i that ranges between -1.01 and 4.93). Bottom right: sites where samples were collected (46 samples in 22 sites; diamond: strain 1; plus: strain 2; triangle: strain 3; circle: strain 4; cross: strain 5). doi:10.1371/journal.pone.0086591.g003

detect any differences between the parameters $z(s)$. Testing the method on simulations will help us in assessing the effect of the bandwidth b for a given amount of information.

Ranking of Pathogen Strains

We use the approximate regression model (3) to rank the pathogen strains in their contributions to natural epidemics. In this model, Z_i is the response variable, $\{\hat{p}_i(1), \dots, \hat{p}_i(S)\}$ is the vector of explanatory variables and $\{z(1), \dots, z(S)\}$ are the regression coefficients. A simple linear regression is then carried out (e.g. using the $lm()$ function of the R statistical software) to obtain point estimates $\hat{z}(s)$ of the coefficients $z(s)$, $s=1, \dots, S$. Then, the coefficients $z(s)$ can be ranked by using their estimated values.

To assess whether the ranking in the coefficients $z(s)$ is significant, we adopted a permutation approach [25]. For B different independent random permutations, say perm_b ($b=1, \dots, B$), of the indices $i \in \{1, \dots, I\}$ for which the proportions $\hat{p}_i(s)$ can be computed, we estimated the coefficients $\{z_b(s) : s=1, \dots, S\}$ of the following model:

$$Z_i = \left(\sum_{s=1}^S \hat{p}_{\text{perm}_b(i)}(s) z_b(s) \right) + \varepsilon_i.$$

Let $\hat{z}_b(s)$ denote the estimate of $z_b(s)$ obtained by fitting the previous model. Then, for two strains s and s' ($s \neq s'$), the p -value of the unilateral difference permutation test $z(s) = z(s')$ versus $z(s) > z(s')$ is: $\frac{1}{B} \sum_{b=1}^B \mathbb{1}\{\hat{z}_b(s) - \hat{z}_b(s') \geq \hat{z}(s) - \hat{z}(s')\}$.

Because several pairwise tests can be carried out when there are more than two strains, the usual significance level 0.05 for a p -value is too high [26]. The simple Bonferroni's correction that consists of dividing the significance level by the number of tests should be very conservative for the null hypothesis because the ranking tests are dependent. However, we will apply this correction and test it on simulations.

Test Data Sets Obtained Under the Regression Model

Our method consists of performing a linear regression with noisy explanatory variables. Thus, the convergence results of classical linear regression do not hold [27]. To assess the effect of using noisy explanatory variables, namely the estimated proportions $\hat{p}_i(s)$, we applied the method to simulated data sets obtained under the regression model (2) but analyzed with the model (3). The technical details and the detailed results are provided in File S1 (Sec. A).

Table 1. Results of the ranking of pathogen strains observed within a natural epidemic of powdery mildew in *Plantago lanceolata*.

Strain	1	2	3	4	5
Number of samples	1	11	13	16	5
	$z(1)$	$z(2)$	$z(3)$	$z(4)$	$z(5)$
Estimated value	-8.16	1.29	1.43	1.88	4.42
		$z(2)>z(1)$	$z(3)>z(1)$	$z(4)>z(1)$	$z(5)>z(1)$
<i>p</i> -value		0.007	0.010	0.008	0.011
			$z(3)>z(2)$	$z(4)>z(2)$	$z(5)>z(2)$
<i>p</i> -value			0.446	0.294	0.078
				$z(4)>z(3)$	$z(5)>z(3)$
<i>p</i> -value				0.238	0.038
					$z(5)>z(4)$
<i>p</i> -value					0.064

The table provides frequencies of strains in the whole sample, estimated values of coefficients $z(s)$, and test *p*-values indicating the significance of the ranking between the pathogen strains. The strains were ordered with respect to the estimated values of $z(s)$.

doi:10.1371/journal.pone.0086591.t001

Test Data Sets Obtained Under a Mechanistic Model

In practice, our method will be applied to data *generated* under mechanistic processes that are more complex than model (2). To assess the effect of using a regression model for the analysis instead of the true mechanistic model, we applied the method to simulated data sets obtained under an original mechanistic model detailed in File S1 (Sec. B). In this model, the epidemic spreads over a 10×10 square grid with inter-node distance equal to one ($I = 100$), and at discrete integer times $t = 1, 2, \dots, T = 7$. The epidemic is the sum of $S = 3$ sub-epidemics corresponding to S strains. The S sub-epidemics are mutually independent. Each sub-epidemic is randomly initiated in time and in intensity. The growth and the spread of the sub-epidemics are governed by Poisson distributions and an exponential dispersal kernel. The spread depends on a dispersal parameter γ that is the same for the S strains. The growth depends on a coefficient β_s that represents the fitness of strain s . The coefficients β_s in the mechanistic model are the counterparts of the coefficient $z(s)$ in the regression model (2).

We carried out 1,600 simulations of the mechanistic model; 800 with the dispersal parameter γ equal to 0.2 (short dispersal distances; see illustration in File S1, Sec. B, Figures S4 and S6), 800 with $\gamma = 0.5$ (longer dispersal distances; see illustration in File S1, Sec. B, Figure S8). Among each series of 800 simulations, 200 were made with equal coefficients: $(\beta_1, \beta_2, \beta_3) = (2.0, 2.0, 2.0)$, 200 with slight differences in the coefficients: $(\beta_1, \beta_2, \beta_3) = (1.9, 2.0, 2.2)$, 200 with intermediate differences: $(\beta_1, \beta_2, \beta_3) = (1.5, 2.0, 3.0)$, and 200 with large differences: $(\beta_1, \beta_2, \beta_3) = (1.0, 2.0, 4.0)$. To study the effect of the sampling effort, different sample sizes were considered for the genetic data: we used different numbers of sampling sites (10, 20 and 30) and different numbers of samples per sampling site (1, 5 and 10); see details in File S1 (Sec. B). For each simulation and each sampling effort, we tested the hypothesis of no difference in the coefficients for each pair of strains (1 and 2; 2 and 3; 1 and 3) by using the unilateral permutation test orientated with respect to the estimated coefficients (e.g. if $\hat{z}(1) > \hat{z}(2)$, we tested $z(1) = z(2)$ versus $z(1) > z(2)$). Then, in each case, we counted

the numbers of adequate and inadequate rejections of the null hypothesis among 200 repetitions.

Computer Code

An R package entitled StrainRanking containing the ranking method, the real data and generators of data under the regression and mechanistic models is available in the CRAN package repository. In this package, the ranking is carried out with the function entitled ranking.strains().

Results

Application to Simulations

The application of the method to simulations performed under the regression model is shown in File S1 (Sec. A; Figures S1, S2, S3; Tables S1, S2). The following general conclusions can be drawn. (i) One rarely rejects the null hypothesis for the wrong alternative hypothesis. (ii) The larger differences between the coefficients $z(s)$ are more often detected than the smaller ones. (iii) Increasing the bandwidth leads to a more powerful test but slightly increases the number of times that the wrong alternative is accepted. (iv) More importantly, the ranking method is efficient despite the use of noisy explanatory variables.

Then, the method was applied to simulations under the mechanistic model. In this case, the model used to analyze the data is definitely different from the model used to simulate the data, but, with our ranking method, we expect to detect a signature of the variation in strain fitness (the signature is the ranking). The contributions of the pathogen strains to the epidemics are measured with the coefficients $(\beta_1, \beta_2, \beta_3)$ in the mechanistic *simulation* model, and with the coefficients $(z(1), z(2), z(3))$ in the regression *analysis* model. The rankings of $(\beta_1, \beta_2, \beta_3)$ and $(z(1), z(2), z(3))$ should be the same. Here, we consider two values (0.2 and 0.5) of the dispersal parameter γ to see in which situation the method is able to detect the variation in strain fitness.

The application of the method to three simulations performed under the mechanistic model (with equal or different coefficients $(\beta_1, \beta_2, \beta_3)$ and with two different values of γ) is detailed in File S1 (Sec. B; Figures S4, S5, S6, S7, S8, S9; Tables S3, S4, S5) where examples of simulated multi-strain dynamics are also displayed. Here, we only provide the results obtained for the series of simulations. For each bandwidth b (0, 1, 2, 3), each sampling effort and each dispersal parameter γ (0.2, 0.5), Figures 1 and 2 show the numbers of times among 200 repetitions that the null hypothesis ($z(s) = z(s')$) was rejected. The rejection threshold was fixed at $0.05/3$, using Bonferroni's correction.

The following conclusions can be drawn. When the dispersal parameter γ is 0.2 (short dispersal), the conclusions are similar to those drawn with the regression model: (i) one rarely rejects the null hypothesis for the wrong alternative hypothesis (white bars); (ii) the larger differences between the coefficients $z(s)$ are more often detected than the smaller ones; (iii) increasing the bandwidth slightly increases the number of times that the wrong alternative is accepted. When the dispersal parameter is 0.5 (long dispersal), the test is less powerful and increasing the bandwidth increases the risk of accepting the wrong alternative hypothesis. Besides, when the differences between the strains are large, the power to detect differences between strain 1 (the less fit) and the other strains is very low. The reason is that, most often, strain 1 has a relatively negligible intensity and is not sampled.

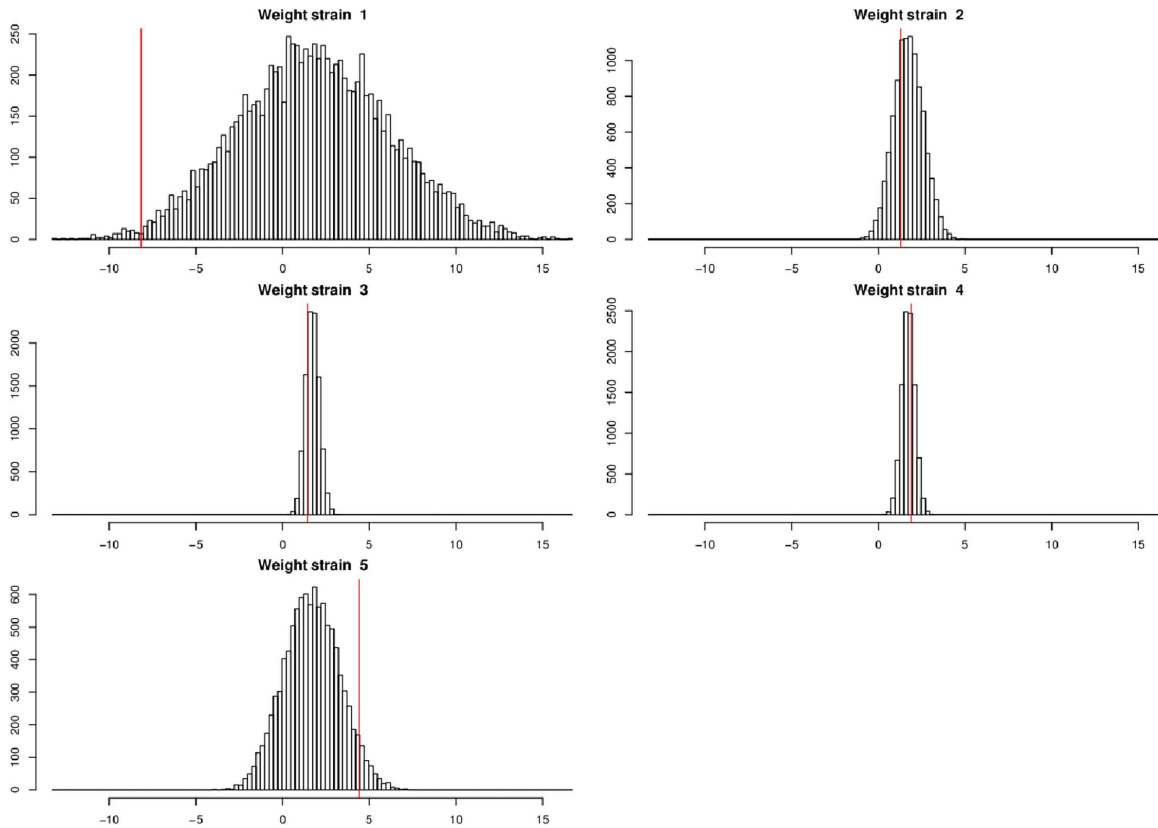


Figure 4. Estimated values of the coefficients $z(s)$ for powdery mildew strains collected in a patch of *Plantago lanceolata* (vertical lines) and corresponding permutation-based distributions obtained under the null hypothesis of coefficient equality (histograms).
doi:10.1371/journal.pone.0086591.g004

Application to Powdery Mildew of *Plantago lanceolata*

The ranking method was applied to the field data of powdery mildew epidemics displayed in Figure 3. Among the 44 collected samples, 40 represented single-strain infections, leading to the identification of five different strains within the pathogen population. Among the four mixed-genotype infections, three could be attributed to a mix of previously identified strains, whereas one remained unattributed and was removed from the dataset. For the analysis, we used the intermediate bandwidth $b=2$ to decrease the risk of detecting false positive differences. In addition, since there are five strains, the total number of unilateral tests is 10 and the rejection threshold is of the order $0.05/10$, using Bonferroni's correction. However, this threshold value is certainly very conservative (tendency to under-reject the null hypothesis of coefficient equality when this hypothesis is wrong).

Table 1 provides the number of samples per strain, the estimated values of the coefficients ($z(1), \dots, z(5)$) and the p -values associated with the unilateral permutation tests. Figure 4 shows the estimated values of the coefficients and their permutation-based distributions under the null hypothesis of coefficient equality. Based on the available data, there is no significant difference in strain fitness at the (certainly too conservative) rejection threshold 0.005 (the relatively low p -values concerning strain 1 have to be considered with caution since there is only one sample corresponding to this strain). Nevertheless, strain 5 tends to have a higher fitness than the other strains and, to be able to conclude in future studies about differences in strain fitness, more genetic samples should be gathered.

Discussion

The method presented here was developed to assign ranks to different pathogen strains with respect to their contribution to natural epidemics. As shown with a simulation-based study, the method can achieve this aim. Importantly, the success of the method depends on the design of the field survey as the statistical power of our approach depends on the sampling size (larger the sample, better the detection of actual differences between strains) and on the sampling scale (large dispersal distances with respect to the spatial extent of the sampling may decrease the power of our approach).

To reach more accurate ranking, the method could be improved as follows. (i) Other growth variables Z_i could lead to a larger statistical power and robustness. We could especially use multidimensional growth variables to handle different features of pathogen spread. We could also build growth variables that depend on the host population to take into account an eventual limiting capacity due to low host densities. (ii) A spatially dependent heteroscedastic and non-stationary noise could replace the white noise in the analysis regression model to take into account the dependence between neighbor cells due to the dispersal of the pathogen. A residual analysis like in [28] and [29] could be carried out to specify the noise structure. (iii) If the observed proportions $p_i^{obs}(s)$ of pathogen strains are not based on the same number of pathogen samples, then the weights w_{ij} could be modified to avoid to give strong weights to strongly uncertain observed proportions. (iv) Finally, an automatic selection of the bandwidth b and the rejection threshold could be developed using

cross-validation or Monte Carlo simulations performed under the fitted regression model.

Disease ecologists commonly use experimental infections in controlled conditions to estimate the fitness of different pathogen strains/genotypes (see for example [17,30–36]). But how the differences between strains found in lab-measured fitness translate to the actual performance in the field has never been assessed to our knowledge. In this study, we developed analytical tools to estimate field performance of pathogen genotypes, allowing further comparison with fitness measures of pathogen strains estimated under controlled conditions. Simple correlations between the two measures for each pathogen genotype may however not be expected if the pathogen genotype interacts with local host genotypes, or with the local environment, to determine the pathogen's fitness [17]. However, such comparisons are useful for estimating how complex the experimental design needs to be if aiming at predicting the pathogen performance under natural conditions.

Our statistical exploratory tool mainly based on regression does not rely on mechanistic assumptions on the pathogen dynamics. Therefore, it can be applied to a wide range of pathogens for which epidemiological and genetic data can be collected during natural epidemics or during experimental epidemics in crop fields.

References

- Anderson RM, May RM (1991) Infectious diseases of humans: dynamics and control. Oxford: Oxford University Press.
- Gilligan CA (2002) An epidemiological framework for disease management. *Advances in botanical research* 38: 1–64.
- Shaw MW (2002) Epidemic modelling and disease forecasting. In: Waller JM, Lenné JM, Waller SJ, editors, *Plant Pathologists' Pocketbook*. Wallingford: CABI Publishing, 252–265.
- Gibson GJ, Gilligan CA, Kleczkowski A (1999) Predicting variability in biological control of a plantpathogen system using stochastic models. *Proceedings of the Royal Society of London Series B: Biological Sciences* 266: 1743–1753.
- Pullan RL, Sturrock HJW, Soares Magalhães RJ, Clements ACA, Brooker SJ (2012) Spatial parasite ecology and epidemiology: a review of methods and applications. *Parasitology* 139: 1870–1887.
- Morens DM, Folkers GK, Fauci AS (2004) The challenge of emerging and re-emerging infectious diseases. *Nature* 430: 242–249.
- Ostfeld RS, Glass GE, Keasing F (2005) Spatial epidemiology: an emerging (or re-emerging) discipline. *Trends in Ecology & Evolution* 20: 328–336.
- Tack AJM, Thrall PH, Barrett LG, Burdon JJ, Laine AL (2012) Variation in infectivity and aggressiveness in space and time in wild host-pathogen systems: causes and consequences. *Journal of Evolutionary Biology* 25: 1918–1936.
- Criscione CD, Poulin R, Blouin MS (2005) Molecular ecology of parasites: elucidating ecological and microevolutionary processes. *Molecular ecology* 14: 2247–2257.
- Giraud T, Enjalbert J, Fournier E, Delmotte F, Dutech C (2008) Population genetics of fungal diseases of plants. *Parasite* 15: 449–454.
- Qi W, Kaser M, Roltgen K, Yeboah-Manu D, Pluschke G (2009) Genomic diversity and evolution of *Mycobacterium ulcerans* revealed by next-generation sequencing. *PLoS pathogens* 5: e1000580.
- Frenkel O, Portillo I, Brewer MT, Peros JP, Cadle-Davidson L, et al. (2012) Development of microsatellite markers from the transcriptome of *Erysiphe necator* for analysing population structure in North America and Europe. *Plant Pathology* 61: 106–119.
- Cui Y, Yu C, Yan Y, Li D, Li Y, et al. (2013) Historical variations in mutation rate in an epidemic pathogen, *Yersinia pestis*. *Proceedings of the National Academy of Sciences* 110: 577–582.
- Archie EA, Luikart G, Ezenwa VO (2009) Infecting epidemiology with genetics: a new frontier in disease ecology. *Trends in Ecology & Evolution* 24: 21–30.
- Thrall PH, Burdon JJ, Bever JD (2002) Local adaptation in the *Linum marginale*-*Melampsora lini* host-pathogen interaction. *Evolution* 56: 1340–1351.
- Luijckx P, Ben-Ami F, Mouton L, Du Pasquier L, Ebert D (2011) Cloning of the unculturable parasite *Pasteuria ramosa* and its *Daphnia* host reveals extreme genotype-genotype interactions. *Ecology letters* 14: 125–131.
- Laine AL (2007) Pathogen fitness components and genotypes differ in their sensitivity to nutrient and temperature variation in a wild plant-pathogen association. *Journal of evolutionary biology* 20: 2371–2378.
- Wolinska J, King KC (2009) Environment can alter selection in host-parasite interactions. *Trends in parasitology* 25: 236–244.
- Tollenaere C, Susi H, Nokso-Koivisto J, Koskinen P, Tack A, et al. (2012) SNP design from 454 sequencing of *Podosphaera plantaginis* transcriptome reveals a genetically diverse pathogen metapopulation with high levels of mixed-genotype infection. *PLoS One* 7: e52492.
- Laine AL, Hanski I (2006) Large-scale spatial dynamics of specialist plant pathogen. *Journal of Ecology* 94: 217–226.
- Soubeyrand S, Laine AL, Penttinen A (2009) Spatio-temporal structure of host-pathogen interactions in a metapopulation. *The American Naturalist* 174: 308–320.
- Ovaskainen O, Laine AL (2006) Inferring evolutionary signals from ecological data in a plantpathogen metapopulation. *Ecology* 87: 880–891.
- Ruppert D, Wand MP, Carroll RJ (2003) *Semiparametric Regression*. Cambridge University Press.
- Silverman BW (1986) *Density Estimation for Statistics and Data Analysis*. London: Chapman and Hall.
- Manly BFJ (1997) *Randomization, Bootstrap and Monte Carlo Methods in Biology*, 2nd Ed. London: Chapman & Hall.
- Miller RG Jr (1981) *Simultaneous Statistical Inference*. New York: Springer-Verlag.
- Carroll RJ, Ruppert D, Stefanski LA, Crainiceanu CM (2006) *Measurement error in nonlinear models: a modern perspective*, volume 105. Chapman & Hall/CRC.
- Soubeyrand S, Chadœuf J, Sache I, Lannou C (2006) Residual-based specification of the random effects distribution for cluster data. *Statistical Methodology* 3: 464–482.
- Soubeyrand S, Chadœuf J (2007) Residual-based specification of a hidden random field included in a hierarchical spatial model. *Computational Statistics and Data Analysis* 51: 6404–6422.
- Bruns E, Carson M, May G (2012) Pathogen and host genotype differently affect pathogen fitness through their effects on different life-history stages. *BMC Evolutionary Biology* 12: 135.
- Grech K, Watt K, Read AF (2006) Host-parasite interactions for virulence and resistance in a malaria model system. *Journal of Evolutionary Biology* 19: 1620–1630.
- Pariaud B, Ravigné V, Halkett F, Goyeau H, Carlier J, et al. (2009) Aggressiveness and its role in the adaptation of plant pathogens. *Plant Pathology* 58: 409–424.
- Salvaudon L, Héraudet V, Shykoff JA (2005) Parasite-host fitness trade-offs change with parasite identity: Genotype-specific interactions in a plant-pathogen system. *Evolution* 59: 2518–2524.
- Smith I (2003) *Mycobacterium tuberculosis* pathogenesis and molecular determinants of virulence. *Clinical microbiology reviews* 16: 463–496.
- Vale PF, Little TJ (2009) Measuring parasite fitness under genetic and thermal variation. *Heredity* 103: 102–109.
- Vojvodic S, Jensen AB, Markussen B, Eilenberg J, Boomsma JJ (2011) Genetic variation in virulence among chalkbrood strains infecting honeybees. *PLoS one* 6: e25035.

To facilitate the application of the method to other pathogens, an open source computer code is available. The code can be modified and extended by the user to meet the user's requirements.

Supporting Information

File S1 Supporting information providing methodological details and complementary results.
(PDF)

Acknowledgments

The authors thanks Coong Lo and Riikka Alanen for performing the field work, Evgeniy Meyke for spatial referencing, the Institute of Biotechnology and the Finnish Institute for Molecular Medicine for DNA extraction and genotyping of the field collected samples.

Author Contributions

Conceived and designed the experiments: CT A-LL EH-L SS. Performed the experiments: CT A-LL. Analyzed the data: SS CT EH-L A-LL. Contributed reagents/materials/analysis tools: SS CT EH-L A-LL. Wrote the paper: SS CT EH-L A-LL.